

Plug-and-Play Transformer Modules for Test-Time Adaptation

Xiangyu Chang¹ Sk Miraj Ahmed¹ Basak Guler¹ Srikanth V. Krishnamurthy¹ Ananthram Swami²
Samet Oymak³ Amit K. Roy-Chowdhury¹

Abstract

Parameter-efficient tuning (PET) methods such as LoRA, Adapter, and Visual Prompt Tuning (VPT) have found success in enabling adaptation to new domains by tuning small *modules* within a transformer model. However, the number of domains encountered during test time can be very large, and the data is usually unlabeled. Thus, adaptation to new domains is challenging; it is also impractical to generate customized tuned modules for each such domain. Toward addressing these challenges, this work introduces PLUTO: a Plug-and-pLay modUlar Test-time adaptatiOn strategy. We pre-train a large set of modules, each specialized for different source domains, effectively creating a “module store”. Given a novel target domain with few-shot unlabeled data, we introduce an unsupervised test-time adaptation (TTA) method to (1) select a sparse subset of relevant modules from this store and (2) create a weighted combination of selected modules without tuning their weights. This plug-and-play nature enables us to harness multiple most-relevant source domains in a single inference call. Comprehensive evaluations demonstrate that *PLUTO uniformly outperforms alternative TTA methods* across several benchmarks and that selecting ≤ 5 modules suffices to extract most of its benefits. At a high level, our method equips pre-trained transformers with the capability to dynamically adapt to new domains, spearheading a new framework for efficient and scalable domain adaptation.

1. Introduction

Pretrained transformers (Devlin et al., 2018; Brown et al., 2020; Liu et al., 2019; Radford et al., 2019; Raffel et al., 2020) have achieved significant recent success, however,

¹University of California, Riverside. Email: {cxian008@, sahme047@, bguler@ece., krish@cs., amitrc@ece.}@ucr.edu

²DEVCOM Army Research Laboratory. Email: ananthram.swami.civ@army.mil

³University of Michigan. Email: oymak@umich.edu

Table 1. Our work compared to the prior art fulfills key criteria for a comprehensive adaptation framework. We adapt with a sample-specific setup and can support few/zero-shot application.

Setting	Source Free	Adaptation On the fly	Dynamic Target	Few/Zero-Shot
UDA	✗	✗	✗	✗
Source-free UDA	✓	✗	✗	✗
TTA	✓	✓	✓	✗
PLUTO	✓	✓	✓	✓

these models are often quite large, with billions of parameters (Brown et al., 2020; Raffel et al., 2020). This has posed challenges for their practical use, especially in edge devices, due to the computational and memory challenges of fine-tuning for downstream tasks. To address this, parameter-efficient tuning (PET) methods have been proposed including prefix/prompt-tuning (Li & Liang, 2021; Lester et al., 2021; Liu et al., 2023), adapter (Houlsby et al., 2019), and LoRA (Hu et al., 2021a). In PET, the pretrained model remains frozen and only the domain-specific (extra) parameters designated for the target domain are updated based on the training data. PET has found notable success as it significantly reduces memory usage and facilitates modular adaptation of the model while often being competitive with fine-tuning.

While PET methods have demonstrated notable benefits across various domains and tasks (Liu et al., 2023; Vu et al., 2021), their effectiveness in more challenging scenarios involving few-shot and unlabeled data or domain shifts remains a major bottleneck (Gu et al., 2021; Raffel et al., 2020). Specifically, we ask: *How to leverage PET methods to adapt to a new domain at test-time (Wang et al., 2020) where we only observe **few-shot unlabeled data** from this new domain?* Here, test-time adaptation (TTA) refers to adapting to new domains during testing, in an online manner, without the need for additional training data. This makes this setting more challenging than standard unsupervised domain adaptation (UDA) (Tsai et al., 2018; Tzeng et al., 2017). TTA typically requires iteratively updating the source model parameters using an unsupervised objective that incorporates the new test sample from the target distribution. Existing test-time adaptation (TTA) techniques mostly depend on a single source model for adaptation (Wang et al.,

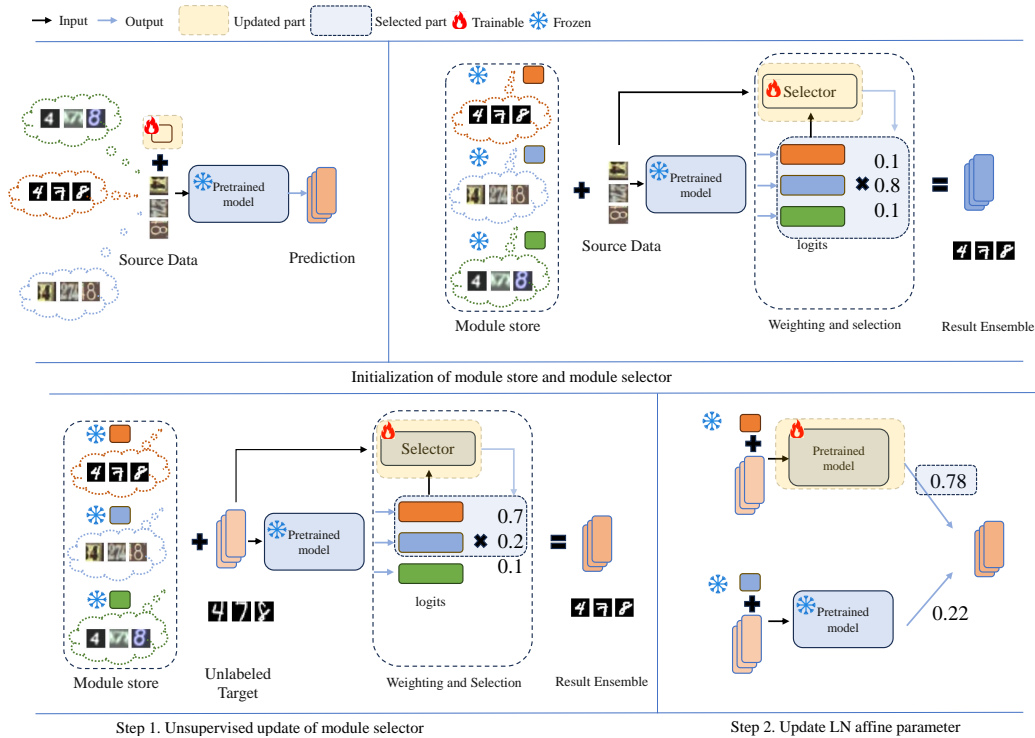


Figure 1. The overview of PLUTO. At test time, PLUTO efficiently combines the sources using appropriate weights determined by the current test distribution. Furthermore, we selectively update the LayerNorm (LN) parameters of the model that demonstrates the highest correlation with the test distribution. The numbers in the figure are examples provided for illustrative purposes.

2020; 2022). However, considering the dynamic nature of the test distribution, it should prove advantageous to adapt a set of source models collectively during test time (Ye et al., 2023; Sun et al., 2015).

In this work, rather than employing multiple distinct source models, we propose to plug source module(s) within a single vision transformer. We naturally cannot expect a single module to work for all target domains. Furthermore, since target domains at test time are few-shot and there can be a large number of domains, it is impractical to train customized PET modules for each target from scratch. Instead, the ideal algorithm should identify the new domain and suitably adapt pre-existing PET modules to this domain. The main contribution of this work is providing a plug-and-play algorithm to address this challenge. We call our method **PLUTO: Plug-and-pLay modUlar Test-time adaptatiOn**.

Concretely, we consider a multi-source domain adaptation setting and propose *pretraining PET modules for a collection of source domains*. These pretrained modules can then be utilized at test-time with minimal supervision and sample size. Importantly, our algorithm PLUTO benefits from having access to a *module store* containing a diverse set of source domains. PLUTO can retrieve the most relevant sources from this *module store* (70+ modules for ImageNet-

C benchmark) and accurately blend them in a target-aware fashion. PLUTO brings three important benefits: (1) *Sample efficiency*: PLUTO enables few-shot unsupervised adaptation in two ways: First, PLUTO only selects and weights a small subset of pretrained modules, rather than tuning a module from scratch, resulting in an efficient search space. Secondly, we utilize an attention-based module selector to identify the most relevant modules to the target domain. This also allows PLUTO to exhibit strong zero-shot adaptation performance. (2) *Anti-forgetting during TTA*: Our plug-and-play use of PET modules and selective update of LayerNorm parameters effectively overcomes the forgetting which is a prominent challenge for TTA methods (see Section. 4.5 for details). (3) *Parameter efficiency*: The adaptation happens through parameter-efficient modules. In a distributed/federated setting where central server operates a *module store*, the clients can efficiently request new modules.

Main Contributions. Overall, our method PLUTO is an effective strategy for harnessing not only a pretrained Vision Transformer (ViT) but also pretrained PET modules within this ViT to enhance few-shot unsupervised TTA performance. Our main technical contributions are:

- **Multi-source PET-based TTA.** To the best of our knowledge, this is the first work to employ multiple

PET modules for the test-time adaptation problem (hence the phrase *plug-and-play*). We not only pretrain a large number of modules, we also present innovative algorithms that can effectively select and blend an optimal subset of these modules to facilitate few-shot unsupervised adaptation to a new domain. Importantly, PLUTO achieves a performance on par with using all modules simultaneously and often outperforms the single best-performing source in hindsight.

- **Algorithmic innovations.** PLUTO facilitates multi-source TTA by weighting the output logits of multiple modules and fine-tuning LayerNorms (LN). Our method crucially captures the relationships between the logit outputs of multiple source modules and input instances with very limited samples and enables PLUTO to decide the contribution of each source domain adaptively on the fly. To ensure the generalizability of the few-shot weight assignment of the source modules, we integrate sharpness-aware minimization and PET methods (Foret et al., 2020) for TTA.
- **Empirical impact and insights.** Comprehensive evaluations on Digits, Office-Home, CIFAR-10C, and ImageNet-C demonstrate that PLUTO uniformly outperforms alternative TTA methods. The performance improvement is much larger in the few-shot setting. For instance, in Office-Home evaluations in Table 5, PLUTO demonstrate **+24% absolute accuracy improvement in zero-shot and 16-shot settings** over the best alternative. To do so, PLUTO typically selects only ≤ 5 modules to extract most of the benefits.

2. Related Works

2.1. Unsupervised Domain Adaptation

Unsupervised Domain Adaptation (UDA) is widely used in various machine learning tasks, including image classification (Tzeng et al., 2017), semantic segmentation (Tsai et al., 2018), object detection (Hsu et al., 2020), and reinforcement learning (Raychaudhuri et al., 2021). These applications address distribution shift challenges by harmonizing source and target domain distributions. Methods utilize techniques like maximum mean discrepancy and adversarial learning (Ganin et al., 2016; Tzeng et al., 2017) for alignment. There is a growing interest in adaptation strategies that rely solely on pretrained source models due to privacy and memory storage concerns regarding source data.

2.2. Test Time Adaptation (TTA)

UDA requires extensive target domain data for offline adaptation, whereas TTA employs a continual, batch-by-batch approach (Valanarasu et al., 2022; Shin et al., 2022; Hu et al., 2021b). Initial studies (Li et al., 2016) adapted using the

current test-batch statistics rather than those from training. TENT (Wang et al., 2020) aims to reduce entropy and updates batch-normalization parameters in a pre-trained source model using new target data. DUA (Mirza et al., 2022) persistently updates batch-norm statistics with incoming test batches for better target domain alignment. A common issue with these approaches is the tendency to forget source knowledge. Methods like CoTTA (Wang et al., 2022) apply stochastic source model restoration to avoid drifting of source knowledge, and EATA (Niu et al., 2022) uses regularization to preserve important weights, thus reducing forgetting. In addition, CLIP (Radford et al., 2021)-based methods (Feng et al., 2023; Shu et al., 2022) adapt to new domains by doing data augmentation and prompt generation. These single-source TTA methods require substantial computational resources to balance the trade-off between adaptation performance and mitigating forgetting. In contrast, by assessing the relevance between multiple source models and the target domain and only updating the most related source models, our approach minimizes forgetting with minimal computational expense while maximizing the utilization of knowledge from all source domains.

2.3. Ensemble learning

Ensemble learning, a well-established approach, aims to create a robust and generalizable model (Hansen & Salamon, 1990). Common ensemble techniques include voting (Hansen & Salamon, 1990), bagging (Breiman, 1996), boosting (Schapire, 1990; Freund & Schapire, 1997), and stacking (Wolpert, 1992). These methods have found applications in various tasks, including model debiasing (Elazar & Goldberg, 2018; Stacey et al., 2020), and domain adaptation (Kim et al., 2017). Apart from considering global domain-to-domain relationships, (Ruder & Plank, 2017; Guo et al., 2018) introduced the use of similarity measures between examples and domains to choose data from various sources for a particular target domain. These selected data are then merged to train a single classifier. Some closely related works to ours are (Kim et al., 2017; Peng et al., 2022), which also incorporate example-to-domain relationships but utilize an attention mechanism. They train the attention module using limited labeled data from the target domain in a supervised manner. In contrast, our method operates in an unsupervised setting and does not rely on such labeled data.

3. Problem Formulation and Proposed Method

We assume access to a pretrained transformer model f . We will build a set of pretrained modules, referred to as *module store*, that can be plugged within f on demand. Let us denote these modules by parameters $\{\theta_j\}_{j=1}^N$ where each θ_j will be trained for a particular source domain. These modules, based on parameter-efficient tuning methods, will

contain much fewer parameters than the base model f . Let us also denote the transformer f with module θ as f_θ . Before describing PLUTO, we introduce our workflow: We will (1) pretrain source modules $\{\theta_j\}_{j=1}^N$ using source datasets and (2) optimally blend these modules for a target task.

- **Pretraining Source Modules:** Given a loss function \mathcal{L} and a fixed set of source domains $\{S_j\}_{j=1}^N$, for each $S \in \{S_j\}_{j=1}^N$, instead of fully fine-tuning ($f \rightarrow f^S$) the pretrained model to the domain S by solving $f^S = \operatorname{argmin}_f \mathcal{L}(f; S)$, given the pretrained model (with modules) f_θ , we freeze the model and only update the module $\theta = \operatorname{argmin}_\theta \mathcal{L}(f_\theta; S)$.
- **Adapt to a new domain:** After obtaining a set of N modules $\{\theta_j\}_{j=1}^N$ corresponding to $\{S_j\}_{j=1}^N$, our objective is to adapt to a new target domain \mathcal{T}_{new} without fine-tuning a new module but only utilizing the current pretrained modules. We aim to find a combination \mathcal{G} of the source models $\mathcal{G}(\{f_{\theta_j}\}_{j=1}^N)$ that minimizes the loss on the new domain:

$$\min_{\mathcal{G}} \mathcal{L}(\mathcal{G}(\{f_{\theta_j}\}_{j=1}^N); \mathcal{T}_{new}).$$

Specifically, \mathcal{G} can be a linear combination of the source models' output. This would apply under the assumption that the target domain distribution can be expressed as the linear combination of source distributions. We'll provide some theoretical insights of this approximation in Appendix F.

Method: To proceed, we provide an overview of PLUTO's framework illustrated in Figure 1. This involves the following steps to achieve unlabeled test-time domain adaptation:

- **(Sec. 3.2) Step 1:** For a test batch at time t , we have both the pretrained modules and the frozen pretrained transformer model. We update the *module selector* \mathcal{G} with pseudo-label entropy minimization. This process helps us learn the module output combination weights and select the most related source modules specific to the current batch. As we discuss in Sections 3.1 and 3.2, *module selector* \mathcal{G} relies on an attention mechanism and plays a crucial role in effectively determining the source modules that are most relevant to the target.
- **(Sec. 3.3) Step 2:** At each time t , we determine which source model is needed to update the LayerNorm (LN) affine parameters by the largest assigned weight from the updated module selector \mathcal{G} .

In both steps, we only require a small number of unlabeled test samples to identify the source modules that are most relevant to the current test batch. We can typically select just a few modules (≤ 5) to achieve performance that approximates the effect of using all weighted source module outputs

Algorithm 1 PLUTO: Plug-and-play Modular Test-time adaptation

- 1: **Input:** Source model with pretrained source modules $\{f_{\theta_j}^j\}_{j=1}^N$, attention-based pretrained module selector \mathcal{G} , number of modules to be selected M ($M < N$), streaming sequential unlabeled test data $\{x_i^{(1)}\}_{i=1}^B \rightarrow \{x_i^{(2)}\}_{i=1}^B \rightarrow \dots \{x_i^{(t)}\}_{i=1}^B \rightarrow \dots$
 - 2: **Output:** M scaled weights, M selected modules, Updated LayerNorm (LN) affine parameters
 - 3: **while** $t \geq 1$ **do**
 - 4: **for** Each x_i in the t -th batch **do**
 - 5: Pass x_i through $\{f_{\theta_j}^j\}_{j=1}^N$
 - 6: Obtain pre-softmax logits $\{l(x_i)^j\}_{j=1}^N$
 - 7: Obtain weights
 - 8: $\{w(x_i)^j\}_{j=1}^N = \mathcal{G}(x_i, \{l(x_i)^j\}_{j=1}^N)$
 - 9: Assign pseudo-label (PL) to x_i
 - 9: **end for**
 - 10: Update $\mathcal{G} \rightarrow \mathcal{G}^*$ with PL entropy minimization on t -th batch (Eqn. 2)
 - 11: Obtain updated weights for all x_i in t -th batch
 - 12: $\forall x_i, \{w^*(x_i)^j\}_{j=1}^N = \mathcal{G}^*(x_i, \{l(x_i)^j\}_{j=1}^N)$
 - 12: Calculate average weights for t -th batch
 - 13: $\{\bar{w}(t)^j\}_{j=1}^N = \overline{\{w^*(x_i)^j\}_{i=1}^B}\}_{j=1}^N$
 - 13: Find and select the top M in $\{\bar{w}(t)^j\}_{j=1}^N$
 - 14: Rescale selected weights to sum up to 1.
 - 15: LN update of source model corresponding to the largest in $\{\bar{w}(t)^j\}_{j=1}^N$ by minimizing Eqn. 4 with Eqn. 8
 - 16: **end while**
-

during forward inference. The pseudocode for PLUTO is provided in Algorithm 1. In what follows, we further elaborate on the design principles of PLUTO.

3.1. Initialization of the Module Selector

Given the correspondence between N source domains S_1, \dots, S_N and their labeled training data, by running parameter-efficient tuning on each domain separately, a set of pretrained modules, or the *module store*, can be obtained: $\{\theta_j\}_{j=1}^N$. Given a certain pretrained transformer model f , we denote the model equipped with different pretrained source modules as $\{f_{\theta_j}^j\}_{j=1}^N$.

For source domains $\{S_j\}_{j=1}^N$ the ground-truth (GT) label of the target sample x is known, and the module selector \mathcal{G} can be initialized by minimizing the cross-entropy loss between the weighted label prediction (will be explained in Sec. 3.2) and the GT label y . As discussed in (Peng et al., 2022), this initialization enables \mathcal{G} to capture the sample-specific preference of different source models.

3.2. Module weighting at test time

Drawing from the success of the attention mechanism in achieving impressive few-shot performance in supervised model ensemble scenarios (Peng et al., 2022; Kim et al., 2017), we design a novel approach to leverage the same during test time adaptation. Even in the unsupervised context of test-time adaptation, we have found that an attention module, which acts as a module selector, can effectively integrate information from multiple source domains into the target domain by dynamically assigning weights and updating them on-the-fly. This enables PLUTO to plug modules from the module store and adapt them at test time with few-shot unlabeled data.

In order to convert a 2D image input into sequential data for the transformer and the module selector to process, the image input $x \in \mathbb{R}^{H \times W \times C}$ is reshaped into a sequence of flattened 2D patches (Dosovitskiy et al., 2020) $\mathbf{X}_p \in \mathbb{R}^{e \times (P^2 \cdot C)}$, where (H, W) is the height and width of the original image, C is the number of channels, (P, P) is the size of each segmented image patch, and $e = HW/P^2$ is number of patches and the effective input sequence length. Assuming that the transformer uses a constant latent vector size d across all of its layers (Dosovitskiy et al., 2020), we flatten the sequence of the patches and map them to d dimensions: $\hat{\mathbf{X}} = [\mathbf{X}_p \mathbf{E}]_{p=1}^N$, $\mathbf{E} \in \mathbb{R}^{(P^2 \cdot C) \times d}$. The patch embedding projection \mathbf{E} is a (frozen) trainable parameter in the pretrained ViT.

The module selector, which is an attention module, gauges the relevance between the output logits of the source modules and instances x_i in the current (t -th) target (abbreviated as T) batch $D_T^{(t)} = \{x_i^{(t)}\}_{i=1}^B$. It then assigns weights based on this relevance. Logits of source models are a function of both the pretrained module and the pretrained transformer and are also capable of modeling the uncertainty in predictions from different sources. We perform max-pooling over the sequence $\hat{\mathbf{X}} = [\mathbf{X}_p \mathbf{E}]_{p=1}^N \in \mathbb{R}^{e \times d}$ and obtain $\hat{x} \in \mathbb{R}^d$ as the representation of the original image input. Furthermore, we pass the input instance x through N pretrained models and obtain pre-softmax logits $\{l(x_i)^j\}_{j=1}^N \in \mathbb{R}^v$. With four trainable parameters: $W_{d,x} \in \mathbb{R}^{d \times d'_x}$, $W_{u,x} \in \mathbb{R}^{d'_x \times d'}$, $W_{d,l} \in \mathbb{R}^{v \times d'_l}$, $W_{u,l} \in \mathbb{R}^{d'_l \times d'}$, the module selector first projects the pre-softmax logits and the representation of the original image input into another representational space: $\mathbf{h}_x = W_{u,x}^\top \cdot \gamma(W_{d,x}^\top \cdot \hat{x})$, $\mathbf{h}_{l,j} = W_{u,l}^\top \cdot \gamma(W_{d,l}^\top \cdot l(x)^j)$. With application of LN (Ba et al., 2016) we are able to obtain the final projected representations $\mathbf{h}_x, \mathbf{h}_{l,j} \in \mathbb{R}^{d'}$ and compute the attention weight $w(x)^j$ to capture the relationship between the input x and its representation from the pretrained models $l(x)^j$:

$$w(x)^j = \mathcal{G}(x_i, \{l(x_i)^j\}_{j=1}^N) = \frac{e^{\mathbf{h}_{l,j} \cdot \mathbf{h}_x}}{\sum_{k=1}^N e^{\mathbf{h}_{l,k} \cdot \mathbf{h}_x}} \quad (1)$$

The ensembled logit is the linear combination of the weighted logits: $l(x) = \sum_{j=1}^N w(x)^j l(x)^j$.

As the GT label of the target sample x is unknown, we denote its pseudo-label, as predicted by source j , as $\hat{y}_j = f_{\theta_j}^j(x)$. We linearly combine these pseudo-labels by attention weights $\{w(x)^j\}_{j=1}^N$ to get the weighted pseudo-label $\hat{y} = \sum_{j=1}^N w(x)^j \hat{y}_j$. Using these weighted pseudo-labels for all the samples in the current (t -th) batch, we calculate the expected Shannon entropy of pseudo-label as:

$$\mathcal{L} = -\mathbf{E}_{\mathcal{D}_T^{(t)}} \sum_{c=1}^K \hat{y}_c \log(\hat{y}_c), \quad (2)$$

where K is the number of classes and \hat{y}_c is the c -th entry of the predicted pseudo-label. By performing entropy minimization on Eqn. 2, we can update the module selector parameters (from \mathcal{G} to \mathcal{G}^*) and obtain updated attention weights for Eqn. 1. Minimization of the Shannon entropy attempts to raise the confidence of an individual sample's prediction and weight assignment (Lee et al., 2023).

3.3. Domain adaptation of LN affine parameters

In TTA, prior methods often conduct adaptation on pre-trained models with batch normalization (BN) layers (Ioffe & Szegedy, 2015) and most of them are built upon BN statistics adaptation (Schneider et al., 2020; Wang et al., 2020; Zhang et al., 2022). However, recent works (Liu et al., 2022; De Min et al., 2023; Kim et al., 2021) found out that layer normalization (LN, (Ba et al., 2016)) can be a better adaptation choice for transformers. Specifically, for the k -th layer with a d -dimensional input $x = (x^{(1)}, \dots, x^{(d)})^\top \in \mathbb{R}^d$, the layer normalized outputs are

$$y^{(k)} = \gamma^{(k)} \hat{x}^{(k)} + \beta^{(k)}, \text{ i.e., } y = \gamma \odot \hat{x} + \beta, \quad (3)$$

where $\hat{x}^{(k)} = \frac{(x^{(k)} - \mu_d)}{\sqrt{\sigma_d^2 + \epsilon_\sigma}}$, $\mu_d = \frac{1}{d} \sum_{k=1}^d x^{(k)}$, $\sigma_d = \frac{1}{d} \sum_{k=1}^d (x^{(k)} - \mu_d)^2$. Here, $\gamma^{(k)}$ and $\beta^{(k)}$ are learnable affine parameters (and we denote them together as λ), ϵ_σ is a small value to ensure numerical convergence. Adaptation to new domains can be achieved by tuning $\gamma^{(k)}$ and $\beta^{(k)}$ in Eqn. 3.

3.3.1. SHARPNESS-AWARE DOMAIN ADAPTATION

While TTA provides stability in LN models, it can lead to model collapse during affine parameter tuning (Eqn. 3). This collapse occurs when the model incorrectly assigns all input samples to a single class over the adaptation process (Niu et al., 2023). To prevent this, we utilize sharpness-aware techniques (Foret et al., 2020; Niu et al., 2023) to make the model less sensitive to large gradients and in test samples (Niu et al., 2022).

Upon obtaining the updated weights from the updated module selector \mathcal{G}^* for each test sample in the target batch $D_T^{(t)} = \{x_i^{(t)}\}_{i=1}^B$ at time step t , we identify the M source modules most relevant to the target batch based on the highest average weights assigned by the module selector. We compute the entropy of the pseudo-labels of current test batch as predicted by these models with pretrained module. The entropy of the prediction of t -th target batch from j -th source model is:

$$\mathcal{L}_j^{(t)} = -\mathbf{E}_{D_T^{(t)}} \sum_{c=1}^K \hat{y}_{jc}^{(t)} \log(\hat{y}_{jc}^{(t)}) \quad (4)$$

We seek to make the model insensitive to the large gradients by encouraging the model to converge to a flat area of the entropy loss surface, since a flat minima has good generalization and robustness to large gradients (Foret et al., 2020; Niu et al., 2023):

$$\min_{\lambda} \mathcal{L}_j^{SA(t)}(\{x_i^{(t)}\}_{i=1}^B; \lambda), \quad (5)$$

$$\text{where } \mathcal{L}_j^{SA(t)} \triangleq \max_{\|\epsilon\|_2 \leq \rho} \mathcal{L}_j^{(t)}(\{x_i^{(t)}\}_{i=1}^B; \lambda + \epsilon) \quad (6)$$

The abbreviation "SA" stands for sharpness-aware. In this context, the inner optimization aims to discover a perturbation ϵ of LayerNorm affine parameters λ within a Euclidean ball of radius ρ that maximizes entropy. The degree of sharpness is measured by the maximum change in the Euclidean ball neighbourhood $N_{\rho}(\lambda)$. This bi-level problem incentivizes the optimization process to locate flat minima. Following SAM (Foret et al., 2020), we can approximately solve the inner optimization via a first-order Taylor expansion,

$$\begin{aligned} \epsilon^*(\lambda) &\triangleq \arg \max_{\|\epsilon\|_2 \leq \rho} \mathcal{L}_j^{(t)}(\{x_i^{(t)}\}_{i=1}^B; \lambda + \epsilon) \\ &\approx \arg \max_{\|\epsilon\|_2 \leq \rho} \mathcal{L}_j^{(t)}(\{x_i^{(t)}\}_{i=1}^B; \lambda) + \epsilon^T \nabla_{\lambda} \mathcal{L}_j^{(t)}(\{x_i^{(t)}\}_{i=1}^B; \lambda) \\ &= \arg \max_{\|\epsilon\|_2 \leq \rho} \epsilon^T \nabla_{\lambda} \mathcal{L}_j^{(t)}(\{x_i^{(t)}\}_{i=1}^B; \lambda) \end{aligned}$$

Denote $\mathbf{v} = \nabla_{\lambda} \mathcal{L}_j^{(t)}(\{x_i^{(t)}\}_{i=1}^B; \lambda)$. Hölder's inequality implies that $\epsilon^T \mathbf{v} \leq \|\epsilon\|_p \|\mathbf{v}\|_q \leq \rho \|\mathbf{v}\|_q (1/p + 1/q = 1)$. For $p = q = 2$, the linear function achieves that bound $\epsilon^*(\lambda)^T \mathbf{v} = \rho \|\mathbf{v}\|_2$, and

$$\epsilon^*(\lambda) = \rho \cdot \text{sgn}(\mathbf{v}) \cdot \frac{|\mathbf{v}|}{\|\mathbf{v}\|_2} \quad (7)$$

By substituting $\epsilon^*(\lambda)$ (Eqn. 7) back into Eqn. 6 and differentiating both sides, the final gradient approximation is:

$$\nabla_{\lambda} \mathcal{L}_j^{SA(t)} \approx \nabla_{\lambda} \mathcal{L}_j^{(t)}(\{x_i^{(t)}\}_{i=1}^B; \lambda)|_{\lambda + \epsilon^*(\lambda)}. \quad (8)$$

By applying Eqn. 8 to update the LN affine parameters of j -th model with Eqn. 4, we can obtain a more reliable solution

Table 2. **Results on Digits.** We train the source modules using 4 digits datasets to perform inference on the remaining dataset ($M = N = 4$). The table clearly shows that the average accuracy of PLUTO outperforms all of the baselines consistently.

Source	Method	MM	MT	UP	SV	SY	Avg
Single	TENT-Best	56.1	98.4	84.9	87.0	95.2	84.3
	TENT-Worst	17.6	54.2	59.6	11.4	15.5	31.7
	CoTTA-Best	55.1	97.5	84.9	86.3	93.6	83.5
	CoTTA-Worst	17.2	54.2	59.7	10.8	15.6	31.5
	EaTA-Best	54.8	97.3	84.2	85.4	93.0	82.9
	EaTA-Worst	16.9	53.4	58.9	10.4	15.8	31.1
Multi	TENT-Ens	62.4	97.8	87.6	55.1	78.4	76.3
	CoTTA-Ens	55.7	97.9	85.7	87.1	95.5	84.4
	EaTA-Ens	55.6	98.0	85.2	85.9	94.9	83.9
	PLUTO (Ours)	63.1	98.9	89.6	87.4	93.7	86.6

Table 3. **Results on Office-Home.** We train the source modules using 3 datasets to perform inference on the remaining dataset ($M = N = 3$). The table clearly shows that the average accuracy of PLUTO outperforms all of the baselines consistently.

Source	Method	Ar	Cl	Pr	Re	Avg
Single	TENT-Best	65.5	51.2	76.8	71.4	66.2
	TENT-Worst	46.6	45.7	56.3	64.0	53.2
	CoTTA-Best	64.4	50.2	76.7	70.5	65.5
	CoTTA-Worst	46.6	46.0	56.0	63.9	53.1
	EaTA-Best	64.8	50.9	77.1	71.4	66.1
	EaTA-Worst	47.4	46.7	55.4	62.8	53.1
Multi	TENT-Ens	63.1	49.2	75.6	71.0	64.7
	CoTTA-Ens	64.6	50.4	76.4	71.7	65.8
	EaTA-Ens	65.8	51.2	76.7	72.6	66.6
	PLUTO (Ours)	66.0	53.6	79.2	76.3	68.7

for entropy minimization. We update the LayerNorm affine parameters for all the layers of j -th source model by back propagating $\mathcal{L}_j^{(t)}$ once, as the approach in (Wang et al., 2020). After updating γ s and β s of LN layers of j -th model, we denote the updated model as $f_{\theta_j}^{j(t)}$ which will be used of the inference on $(t + 1)$ -th target test batch. This implies $f_{\theta_j}^{j(t+1)} = f_{\theta_j}^{j(t)}$.

4. Evaluations

In the main paper, we employ parameter-efficient fine-tuning (PET) in the form of VPT (Jia et al., 2022; Gao et al., 2022) as our module to demonstrate the effectiveness of our approach. We showcase our method's application to other PET modules in the Appendix Sec. C to illustrate the generality of our approach. The effectiveness of our approach is evaluated on both stationary and continuous test time adaptation benchmarks. During the testing phase, we evaluate our approach under two scenarios: (1) Test batches are sampled from a stationary distribution (2) Test batches are sampled from an evolving dynamic distribution.

Datasets. We demonstrated the efficacy of our approach in handling stationary distributions by assessing its performance on the following domain adaptation benchmarks.

Table 4. **Results on Digits.** Different number of few-shot target samples for training the module selector and tuning the LayerNorm affine parameters.

Data Size	Method	MM	MT	UP	SV	SY	Avg
128	TENT-Ens	62.4	97.8	87.6	55.1	78.4	76.3
	CoTTA-Ens	55.7	97.9	85.7	87.1	95.5	84.4
	EaTA-Ens	55.6	98.0	85.2	85.9	94.9	83.9
	PLUTO	63.1	98.9	89.6	86.4	93.7	86.4
64	TENT-Ens	53.8	89.5	79.2	43.3	67.4	66.6
	CoTTA-Ens	45.1	89.9	77.6	75.3	87.3	75.0
	EaTA-Ens	43.7	87.1	73.5	76.0	86.6	73.4
	PLUTO	59.8	94.6	86.5	81.8	88.3	82.2
16	TENT-Ens	47.8	84.2	73.0	37.6	60.5	60.6
	CoTTA-Ens	38.3	82.4	71.5	68.8	82.0	68.6
	EaTA-Ens	38	81.1	67.7	70.3	81.6	67.7
	PLUTO	55.6	90.2	81.0	77.0	83.1	77.4
Zero-shot	TENT-Ens	41.5	78.1	66.6	29.4	53.9	53.9
	CoTTA-Ens	28.6	76.3	64.8	60.9	73.3	60.8
	EaTA-Ens	28.6	71.9	58.5	61.8	72.9	58.8
	PLUTO	51.5	84.6	73.8	71.8	76.6	71.7

Table 5. **Results on Office-Home.** Different number of few-shot target samples for training the module selector and tuning the LayerNorm affine parameters.

Data Size	Method	Ar	Cl	Pr	Re	Avg
128	TENT-Ens	63.1	49.2	75.6	71.0	64.7
	CoTTA-Ens	64.6	50.4	76.4	71.7	65.8
	EaTA-Ens	65.8	51.2	76.7	72.6	66.6
	PLUTO	66.0	53.6	79.2	76.3	68.7
64	TENT-Ens	49.9	33.9	62.9	54.0	50.2
	CoTTA-Ens	49.6	34.2	61.0	58.8	50.9
	EaTA-Ens	51.4	35.9	62.8	58.7	52.2
	PLUTO	59.7	47.5	71.7	70.2	62.3
16	TENT-Ens	31.5	15.0	47.6	37.4	32.9
	CoTTA-Ens	32.4	17.7	42.2	43.6	34.0
	EaTA-Ens	34.9	17.7	44.2	40.7	34.4
	PLUTO	55.9	44.3	67.8	66.4	58.6
Zero-shot	TENT-Ens	27.8	11.4	44.3	34.3	29.5
	CoTTA-Ens	29.0	13.9	38.8	39.8	30.4
	EaTA-Ens	30.9	13.7	41.0	37.2	30.7
	PLUTO	52.4	40.9	63.9	62.4	54.9

- *Digits-Five.* (Peng et al., 2019) consists of five-digit datasets: MNIST (MT), MNIST-M (MM), USPS (UP), SVHN (SV), and Synthetic Digits (SY). There are 10 classes corresponding to digits ranging from 0 to 9. We employed four of the domains as sources and reserved the remaining domain for testing.
- *Office-Home.* (Venkateswara et al., 2017) The Office-Home dataset consists of four domains: Art (Ar), Clupart (Cl), Product (Pr), and Real World (Re), each containing 65 classes. For evaluating our method in the test-time adaptation scenario, we selected three of these domains as source domains and used the remaining domain as the test data.
- *ImageNet-C.* (Hendrycks & Dietterich, 2019) ImageNet-C dataset consists of 15 diverse corruption types applied to images of ImageNet (Deng et al.,

2009). It consists of algorithmically generated corruptions with 5 severity levels. We regard different corruptions with different severity level as different domains. Thus we will have $5 \times 15 = 75$ domains at most.

In the context of dynamic test distribution, we employ the following benchmarks.

- *CIFAR-100C.* (Hendrycks & Dietterich, 2019) The CIFAR-100 (Krizhevsky et al., 2009) dataset is an image classification dataset consisting of 50,000 training images and 10,000 test images. Based on CIFAR-100, CIFAR-100C (Hendrycks & Dietterich, 2019) introduced 15 different types of noise at different severity levels (1 \rightarrow 5). This dataset has since been utilized in various studies on continuous test-time adaptation.

4.1. Baseline Methods

Our evaluation includes comparisons with widely recognized single-source test-time adaptation methods, notably TENT (Wang et al., 2020), CoTTA (Wang et al., 2022), and EATA (Niu et al., 2022). These methods represent the current state-of-the-art (SOTA) in this area. We adopt a setup similar to that in (Ahmed et al., 2021), applying each source model individually to specific test domain data. This approach generates **Best** and **Worst** outcomes, corresponding to the highest and lowest performance achieved among the source models when adapted using a certain method, respectively. We also generalize these single-source adaptation methods into multi-source by uniformly averaging pre-softmax logits of all sources’ outputs given a target sample to make the prediction. The results of uniformly averaged Ensemble of multiple single sources methods are reported.

4.2. Implementation details

We use ViT-Base-16 (Dosovitskiy et al., 2020) model pre-trained on JFT-300M dataset for all our experiments. For all experiments, we use a target batch size of $B = 128$, as used by TENT (Wang et al., 2020). Further details on the experimental settings are provided in Appendix D.

4.3. Object recognition and digit classification

We report the results of object recognition on Office-home (Venkateswara et al., 2017) and Digits-Five (Peng et al., 2019) datasets in Table. 2, 3. We compute the accuracy for each incoming test batch and subsequently present the results by averaging the accuracy values across all the batches. For Office-home dataset, the number of source modules is $N = 3$, and we use all $M = N$ (in Alg. 1) to do the inference on the target domain. A similar setup was used for

Table 6. **Results CIFAR-10C.** We take $M = N = 4$ source modules trained on *Snow*, *Frost*, *Fog*, and *Bright*. We employ these models for adaptation on 15 sequential target domains (severity level=1).

	GN	SN	IN	DB	FGB	MB	ZB	Snow	Frost	Fog	Bright	Contrast	Elastic	Pixel	JPEG	Avg
CoTTA-Best	58.0	59.3	43.9	54.6	45.7	43.0	43.8	37.0	36.1	27.5	29.0	14.3	14.4	12.9	9.7	35.3
EaTA-Best	55.2	57.6	45.5	66.7	58.5	66.3	69.3	69.7	72.9	70.6	69.2	67.4	62.6	68.1	52.4	63.5
TENT-Best	52.4	55.6	46.0	70.1	61.4	68	68.5	68.2	70.9	71.0	71.5	68.7	67.8	69.5	61.9	64.8
CoTTA-Ens	58.4	61.3	42.5	57.0	45.1	44.5	45	38.5	36.0	26.7	27.4	15.4	14.9	12.8	8.2	35.6
EaTA-Ens	56.2	58.5	46.7	69.2	56.6	68.3	70.4	69.2	75.5	71.5	68.9	69.9	64.7	67.1	53.8	64.4
TENT-Ens	53.6	57.7	45.8	71.9	59.5	68.4	68.8	69.5	72.2	70.5	69.7	69.7	67.8	69.7	62.4	65.1
PLUTO	61.6	63.3	48.7	75.2	64.9	71.8	73.7	73.0	78.9	75.0	74.9	73.2	70.5	72.8	65.0	69.5

Table 7. **Results on ImageNet-C.** PLUTO adaptation with top k favorable source modules. k stands for the number of used PET source modules in PLUTO, w.r.t the assigned weight. We adapt 15 target domains (severity level=1) separately.

Method	k	GN	SN	IN	DB	GB	MB	ZB	Snow	Frost	Fog	Bright	Contrast	Elastic	Pixel	JPEG	Avg
PLUTO	1	66.2	75.4	76	74.9	74.9	77.2	75.9	75.2	76.6	76.4	76.3	76.3	75.1	77.2	76.8	75.4
	3	69.8	78.3	78.7	77.6	76.9	79.5	77.9	77.6	79.3	79.2	78.6	79.3	77.7	79.4	79.3	77.9
	5	72.3	78.9	79.2	78.3	77.9	80.3	78.2	78.1	80.4	80.5	79.2	80.0	78.1	79.9	79.7	78.7
	15	72.7	79.3	79.7	78.7	78.3	80.9	78.8	78.8	81.0	80.8	79.8	80.5	78.6	80.4	80.4	79.2
	75	72.8	79.5	80.1	78.9	78.5	81.1	79.1	79.0	81.3	81.0	80.0	80.7	78.8	80.5	80.5	79.4

Digits-Five dataset, except $M = N = 4$ here.

4.4. Few-shot adaptation

Our default setting follows existing studies(Wang et al., 2020) by using 128 few-shot labeled data for each target task, as per the target batch size (B), to update the LN affine parameters and the module selector. Our interest lies in examining how PLUTO’s performance changes with varying shots ($U \leq B$) compared to other techniques. The outcomes are displayed in Table. 4 and Table. 5. We observe that PLUTO consistently outperforms existing TTA methods’ uniform ensemble across various amounts of few-shot unlabeled target data. It suggests that PLUTO can be applied to a wide range of few-shot settings. Even in zero-shot settings PLUTO can outperform other methods, since PLUTO benefits from its sample-specific adaptation strategy.

4.5. Forgetting issue

We extensively experiment with CIFAR-10C dataset to assess our model’s performance in the face of dynamic test distributions. Our method’s resistance to catastrophic forgetting is showcased by measuring classification accuracy on the original source test set after adapting to each domain (Niu et al., 2022; Song et al., 2023). For PLUTO, our ensemble method is employed during domain adaptation, and post-adaptation, each adapted source model is tested on its specific source test set. Regarding the baseline single-source methods and their average ensembles, each model is individually adapted to the new domain and then tested on its respective source test set. The reported accuracy in Table. 6 is the average derived from all these individually adapted single-source models. PLUTO serves an optimal aggregation of source models as well as better preservation of source knowledge.

4.6. Module selection

In previous experiments, we use all the source modules without selection for the target domains as mentioned earlier, regardless of their actual transferability given the target domain. However, if a source domain is too different from the target domain, it is possible that this source task wouldn’t effect the target task positively in general. In order to investigate how PLUTO performs when less preferable source domains are added, we conduct experiments as follows:

On ImageNet-C dataset, we pretrain a module store of 75 modules($N = 75$ in Alg. 1), each corresponding to a domain. We test PLUTO by choosing $M = k$ modules based on the module selector weight assignment for each module. The results presented in Table. 7, suggest that PLUTO effectively identifies target samples where less favored source tasks excel and appropriately adjusts sample-specific weights. This ability to rely more on these source models for certain target samples highlights the efficiency of PLUTO’s sample-specific approach.

5. Conclusion

PLUTO, our Test Time Adaptation (TTA) algorithm for transformers, adaptively combines several source parameter-efficient tuning (PET) modules during testing. Our experiments highlight PLUTO’s three key advantages: (1) Its adaptation strategy, which leverages multiple source domains, utilizes diverse domain knowledge for enhanced performance. (2) The sample-specific TTA approach of PLUTO contributes to its strong few-shot performance. (3) The use of PET modules for minimal parameter updates during test time prevents catastrophic forgetting. On multiple datasets, we demonstrate the power of our proposed approach, especially in a few-shot setting, and with a small number of selected modules.

Impact Statement

This paper presents a framework where a user can effectively adapt their machine learning model to their own needs by downloading modules from a global database. Thus, the outcomes of this work will potentially allow large transformer-based models to be applied to devices with limited computation power, e.g., those at the edge.

References

- Ahmed, S. M., Raychaudhuri, D. S., Paul, S., Oymak, S., and Roy-Chowdhury, A. K. Unsupervised multi-source domain adaptation without access to source data. In *Proceedings of the IEEE/CVF conference on computer vision and pattern recognition*, pp. 10103–10112, 2021.
- Ba, J. L., Kiros, J. R., and Hinton, G. E. Layer normalization. *arXiv preprint arXiv:1607.06450*, 2016.
- Baevski, A. and Auli, M. Adaptive input representations for neural language modeling. *arXiv preprint arXiv:1809.10853*, 2018.
- Breiman, L. Bagging predictors. *Machine learning*, 24: 123–140, 1996.
- Brown, T., Mann, B., Ryder, N., Subbiah, M., Kaplan, J. D., Dhariwal, P., Neelakantan, A., Shyam, P., Sastry, G., Askell, A., et al. Language models are few-shot learners. *Advances in neural information processing systems*, 33: 1877–1901, 2020.
- De Min, T., Mancini, M., Alahari, K., Alameda-Pineda, X., and Ricci, E. On the effectiveness of layernorm tuning for continual learning in vision transformers. *arXiv preprint arXiv:2308.09610*, 2023.
- Deng, J., Dong, W., Socher, R., Li, L.-J., Li, K., and Fei-Fei, L. Imagenet: A large-scale hierarchical image database. In *2009 IEEE conference on computer vision and pattern recognition*, pp. 248–255. Ieee, 2009.
- Devlin, J., Chang, M.-W., Lee, K., and Toutanova, K. Bert: Pre-training of deep bidirectional transformers for language understanding. *arXiv preprint arXiv:1810.04805*, 2018.
- Dosovitskiy, A., Beyer, L., Kolesnikov, A., Weissenborn, D., Zhai, X., Unterthiner, T., Dehghani, M., Minderer, M., Heigold, G., Gelly, S., et al. An image is worth 16x16 words: Transformers for image recognition at scale. *arXiv preprint arXiv:2010.11929*, 2020.
- Elazar, Y. and Goldberg, Y. Adversarial removal of demographic attributes from text data. *arXiv preprint arXiv:1808.06640*, 2018.
- Feng, C.-M., Yu, K., Liu, Y., Khan, S., and Zuo, W. Diverse data augmentation with diffusions for effective test-time prompt tuning. In *Proceedings of the IEEE/CVF International Conference on Computer Vision*, pp. 2704–2714, 2023.
- Foret, P., Kleiner, A., Mobahi, H., and Neyshabur, B. Sharpness-aware minimization for efficiently improving generalization. *arXiv preprint arXiv:2010.01412*, 2020.
- Freund, Y. and Schapire, R. E. A decision-theoretic generalization of on-line learning and an application to boosting. *Journal of computer and system sciences*, 55(1):119–139, 1997.
- Ganin, Y., Ustinova, E., Ajakan, H., Germain, P., Larochelle, H., Laviolette, F., Marchand, M., and Lempitsky, V. Domain-adversarial training of neural networks. *The journal of machine learning research*, 17(1):2096–2030, 2016.
- Gao, Y., Shi, X., Zhu, Y., Wang, H., Tang, Z., Zhou, X., Li, M., and Metaxas, D. N. Visual prompt tuning for test-time domain adaptation. *arXiv preprint arXiv:2210.04831*, 2022.
- Gu, Y., Han, X., Liu, Z., and Huang, M. Ppt: Pre-trained prompt tuning for few-shot learning. *arXiv preprint arXiv:2109.04332*, 2021.
- Guo, J., Shah, D. J., and Barzilay, R. Multi-source domain adaptation with mixture of experts. *arXiv preprint arXiv:1809.02256*, 2018.
- Hansen, L. K. and Salamon, P. Neural network ensembles. *IEEE transactions on pattern analysis and machine intelligence*, 12(10):993–1001, 1990.
- Hendrycks, D. and Dietterich, T. Benchmarking neural network robustness to common corruptions and perturbations. *arXiv preprint arXiv:1903.12261*, 2019.
- Houlsby, N., Giurgiu, A., Jastrzebski, S., Morrone, B., De Laroussilhe, Q., Gesmundo, A., Attariyan, M., and Gelly, S. Parameter-efficient transfer learning for nlp. In *International Conference on Machine Learning*, pp. 2790–2799. PMLR, 2019.
- Hsu, H.-K., Yao, C.-H., Tsai, Y.-H., Hung, W.-C., Tseng, H.-Y., Singh, M., and Yang, M.-H. Progressive domain adaptation for object detection. In *Proceedings of the IEEE/CVF winter conference on applications of computer vision*, pp. 749–757, 2020.
- Hu, E. J., Shen, Y., Wallis, P., Allen-Zhu, Z., Li, Y., Wang, S., Wang, L., and Chen, W. Lora: Low-rank adaptation of large language models. *arXiv preprint arXiv:2106.09685*, 2021a.

- Hu, M., Song, T., Gu, Y., Luo, X., Chen, J., Chen, Y., Zhang, Y., and Zhang, S. Fully test-time adaptation for image segmentation. In *Medical Image Computing and Computer Assisted Intervention—MICCAI 2021: 24th International Conference, Strasbourg, France, September 27–October 1, 2021, Proceedings, Part III 24*, pp. 251–260. Springer, 2021b.
- Ioffe, S. and Szegedy, C. Batch normalization: Accelerating deep network training by reducing internal covariate shift. In *International conference on machine learning*, pp. 448–456. pmlr, 2015.
- Jia, M., Tang, L., Chen, B.-C., Cardie, C., Belongie, S., Hariharan, B., and Lim, S.-N. Visual prompt tuning. In *European Conference on Computer Vision*, pp. 709–727. Springer, 2022.
- Kim, K., Laskin, M., Mordatch, I., and Pathak, D. How to adapt your large-scale vision-and-language model. 2021.
- Kim, Y.-B., Stratos, K., and Kim, D. Domain attention with an ensemble of experts. In *Proceedings of the 55th Annual Meeting of the Association for Computational Linguistics (Volume 1: Long Papers)*, pp. 643–653, 2017.
- Krizhevsky, A., Hinton, G., et al. Learning multiple layers of features from tiny images. 2009.
- Lee, J., Das, D., Choo, J., and Choi, S. Towards open-set test-time adaptation utilizing the wisdom of crowds in entropy minimization. In *Proceedings of the IEEE/CVF International Conference on Computer Vision*, pp. 16380–16389, 2023.
- Lester, B., Al-Rfou, R., and Constant, N. The power of scale for parameter-efficient prompt tuning. *arXiv preprint arXiv:2104.08691*, 2021.
- Li, X. L. and Liang, P. Prefix-tuning: Optimizing continuous prompts for generation. *arXiv preprint arXiv:2101.00190*, 2021.
- Li, Y., Wang, N., Shi, J., Liu, J., and Hou, X. Revisiting batch normalization for practical domain adaptation. *arXiv preprint arXiv:1603.04779*, 2016.
- Liu, X., Zheng, Y., Du, Z., Ding, M., Qian, Y., Yang, Z., and Tang, J. Gpt understands, too. *AI Open*, 2023.
- Liu, Y., Ott, M., Goyal, N., Du, J., Joshi, M., Chen, D., Levy, O., Lewis, M., Zettlemoyer, L., and Stoyanov, V. Roberta: A robustly optimized bert pretraining approach. *arXiv preprint arXiv:1907.11692*, 2019.
- Liu, Z., Mao, H., Wu, C.-Y., Feichtenhofer, C., Darrell, T., and Xie, S. A convnet for the 2020s. In *Proceedings of the IEEE/CVF conference on computer vision and pattern recognition*, pp. 11976–11986, 2022.
- Mirza, M. J., Micorek, J., Possegger, H., and Bischof, H. The norm must go on: Dynamic unsupervised domain adaptation by normalization. In *Proceedings of the IEEE/CVF Conference on Computer Vision and Pattern Recognition*, pp. 14765–14775, 2022.
- Niu, S., Wu, J., Zhang, Y., Chen, Y., Zheng, S., Zhao, P., and Tan, M. Efficient test-time model adaptation without forgetting. In *International conference on machine learning*, pp. 16888–16905. PMLR, 2022.
- Niu, S., Wu, J., Zhang, Y., Wen, Z., Chen, Y., Zhao, P., and Tan, M. Towards stable test-time adaptation in dynamic wild world. *arXiv preprint arXiv:2302.12400*, 2023.
- Peng, X., Bai, Q., Xia, X., Huang, Z., Saenko, K., and Wang, B. Moment matching for multi-source domain adaptation. In *Proceedings of the IEEE/CVF international conference on computer vision*, pp. 1406–1415, 2019.
- Peng, X., Xing, C., Choubey, P. K., Wu, C.-S., and Xiong, C. Model ensemble instead of prompt fusion: a sample-specific knowledge transfer method for few-shot prompt tuning. *arXiv preprint arXiv:2210.12587*, 2022.
- Radford, A., Wu, J., Child, R., Luan, D., Amodei, D., Sutskever, I., et al. Language models are unsupervised multitask learners. *OpenAI blog*, 1(8):9, 2019.
- Radford, A., Kim, J. W., Hallacy, C., Ramesh, A., Goh, G., Agarwal, S., Sastry, G., Askell, A., Mishkin, P., Clark, J., et al. Learning transferable visual models from natural language supervision. In *International conference on machine learning*, pp. 8748–8763. PMLR, 2021.
- Raffel, C., Shazeer, N., Roberts, A., Lee, K., Narang, S., Matena, M., Zhou, Y., Li, W., and Liu, P. J. Exploring the limits of transfer learning with a unified text-to-text transformer. *The Journal of Machine Learning Research*, 21(1):5485–5551, 2020.
- Raychaudhuri, D. S., Paul, S., Vanbaar, J., and Roy-Chowdhury, A. K. Cross-domain imitation from observations. In *International Conference on Machine Learning*, pp. 8902–8912. PMLR, 2021.
- Ruder, S. and Plank, B. Learning to select data for transfer learning with bayesian optimization. *arXiv preprint arXiv:1707.05246*, 2017.
- Schapire, R. E. The strength of weak learnability. *Machine learning*, 5:197–227, 1990.
- Schneider, S., Rusak, E., Eck, L., Bringmann, O., Brendel, W., and Bethge, M. Improving robustness against common corruptions by covariate shift adaptation. *Advances in neural information processing systems*, 33: 11539–11551, 2020.

- Shin, I., Tsai, Y.-H., Zhuang, B., Schuler, S., Liu, B., Garg, S., Kweon, I. S., and Yoon, K.-J. Mm-tta: multi-modal test-time adaptation for 3d semantic segmentation. In *Proceedings of the IEEE/CVF Conference on Computer Vision and Pattern Recognition*, pp. 16928–16937, 2022.
- Shu, M., Nie, W., Huang, D.-A., Yu, Z., Goldstein, T., Anandkumar, A., and Xiao, C. Test-time prompt tuning for zero-shot generalization in vision-language models. *Advances in Neural Information Processing Systems*, 35:14274–14289, 2022.
- Song, J., Lee, J., Kweon, I. S., and Choi, S. Ecotta: Memory-efficient continual test-time adaptation via self-distilled regularization. In *Proceedings of the IEEE/CVF Conference on Computer Vision and Pattern Recognition*, pp. 11920–11929, 2023.
- Stacey, J., Minervini, P., Dubossarsky, H., Riedel, S., and Rocktäschel, T. Avoiding the hypothesis-only bias in natural language inference via ensemble adversarial training. *arXiv preprint arXiv:2004.07790*, 2020.
- Sun, S., Shi, H., and Wu, Y. A survey of multi-source domain adaptation. *Information Fusion*, 24:84–92, 2015.
- Tsai, Y.-H., Hung, W.-C., Schuler, S., Sohn, K., Yang, M.-H., and Chandraker, M. Learning to adapt structured output space for semantic segmentation. In *Proceedings of the IEEE conference on computer vision and pattern recognition*, pp. 7472–7481, 2018.
- Tzeng, E., Hoffman, J., Saenko, K., and Darrell, T. Adversarial discriminative domain adaptation. In *Proceedings of the IEEE conference on computer vision and pattern recognition*, pp. 7167–7176, 2017.
- Valanarasu, J. M. J., Guo, P., VS, V., and Patel, V. M. On-the-fly test-time adaptation for medical image segmentation. *arXiv preprint arXiv:2203.05574*, 2022.
- Venkateswara, H., Eusebio, J., Chakraborty, S., and Panchanathan, S. Deep hashing network for unsupervised domain adaptation. In *Proceedings of the IEEE conference on computer vision and pattern recognition*, pp. 5018–5027, 2017.
- Vu, T., Lester, B., Constant, N., Al-Rfou, R., and Cer, D. Spot: Better frozen model adaptation through soft prompt transfer. *arXiv preprint arXiv:2110.07904*, 2021.
- Wang, D., Shelhamer, E., Liu, S., Olshausen, B., and Darrell, T. Tent: Fully test-time adaptation by entropy minimization. *arXiv preprint arXiv:2006.10726*, 2020.
- Wang, Q., Fink, O., Van Gool, L., and Dai, D. Continual test-time domain adaptation. In *Proceedings of the IEEE/CVF Conference on Computer Vision and Pattern Recognition*, pp. 7201–7211, 2022.
- Wolpert, D. H. Stacked generalization. *Neural networks*, 5(2):241–259, 1992.
- Ye, H., Xie, Q., and Ng, H. T. Multi-source test-time adaptation as dueling bandits for extractive question answering. *arXiv preprint arXiv:2306.06779*, 2023.
- Zhang, M., Levine, S., and Finn, C. Memo: Test time robustness via adaptation and augmentation. *Advances in Neural Information Processing Systems*, 35:38629–38642, 2022.

Appendix Overview

- Section A Sharpness-aware domain adaptation
- Section B Parameter efficiency
- Section C Details on different PET methods
- Section D Hyperparameters
- Section E Details of dataset corruptions
- Section F Theoretical insights

A. Sharpness-aware domain adaptation

Following (Niu et al., 2023), in addition to minimizing the weighted pseudo-label entropy with Eqn. 8, we also seek to filter the samples that of large entropy value. As filtering samples based on their gradient norms directly is impractical, our approach focuses on examining the connection between entropy loss and gradient norms. We aim to eliminate samples with large gradients by considering their entropy values. The entropy is determined by the number of output classes, denoted as K , and it falls within the range $(0, \ln K)$ for various models and datasets. Consequently, selecting a threshold for filtering samples based on their entropy is a more manageable task. The threshold E_0 is set to $0.4 \ln K$ by following EATA (Niu et al., 2022). ρ in Eqn. 7 is set by the default value 5×10^{-2} in (Foret et al., 2020). We provide a overall view of the sharpness-aware DA applied in our method, PLUTO.

Algorithm 2 Sharpness-Aware Test-Time Entropy Minimization

- 1: **Input:** t -th target samples $D_T^{(t)} = \{x_i^{(t)}\}_{i=1}^B$, j -th source model f_λ^j with tunable LN affine parameters λ , step size $\eta > 0$, neighbourhood size $\rho > 0$, entropy threshold E_0 ,
 - 2: **Output:** updated LN parameter λ^*
 - 3: **for** Each $x_i^{(t)}$ in $D_T^{(t)}$ **do**
 - 4: Predict pseudo-label $\hat{y}_i^{(t)} = f_\lambda^j(x_i^{(t)})$
 - 5: Compute entropy $\mathcal{E}_i^{(t)}$
 $\mathcal{E}_i^{(t)}(x_i^{(t)}; \lambda) = -\sum_{c=1}^K \hat{y}_{ic}^{(t)} \log(\hat{y}_{ic}^{(t)})$
 - 6: **if** $\mathcal{E}_i^{(t)} > E_0$ **then**
 - 7: **continue** //filter the sample with large entropy
 - 8: **end if**
 - 9: Compute gradient $\mathbf{v}_i = \nabla_\lambda \mathcal{E}_i^{(t)}(x_i^{(t)}; \lambda)$
 - 10: Compute $\epsilon_i^*(\lambda) = \rho \text{sgn}(\mathbf{v}_i) \frac{\|\mathbf{v}_i\|}{\|\mathbf{v}_i\|_2}$
 - 11: Compute gradient approximation:
 $\mathbf{g}_i = \nabla_\lambda \mathcal{E}_i^{(t)}(x_i^{(t)}; \lambda)|_{\lambda + \epsilon_i^*(\lambda)}$
 - 12: Update $\lambda \leftarrow \lambda - \eta \mathbf{g}_i$
 - 13: **end for**
-

By applying Alg. 2, we minimize Eqn. 4 with Eqn. 8. On

Table A. **Results on Office-Home.** We train the source modules using 3 datasets to perform inference on the remaining dataset.

Source	Method	Ar	Cl	Pr	Re	Avg
Baseline (In Main paper)	TENT-Ens	63.1	49.2	75.6	71.0	64.7
	PLUTO	66.0	53.6	79.2	76.3	68.7
Variants of PLUTO	Module selection	63.4	50.1	76.1	73.4	65.8
	+ SA	65.1	52.9	78.3	75.6	67.9
	+ Filter	63.7	51.5	76.8	74.1	66.3

Table B. Number of parameters for different models' scales and their corresponding PET module size in our setting. ViT-T/S/B/L stands for "Tiny, Small, Base, Large", corresponding to different pretrained ViT sizes. The bolded numbers are the size of the PET modules we applied in our experiments. We highlighted the two size of PET modules in our experiments.

	ViT-T	ViT-S	ViT-B	ViT-L
Full model	5,543,716	21,704,164	85,875,556	303,404,132
Adapter	58,564	116,932	233,668	417,984
VPT	37,732	75,364	150,628	299,108
Header	19,300	38,500	76,900	102,500

Office-Home dataset, we provide an ablation study of how much each component contribute to the performance in Table. A (Here, we apply VPT as the PET module, same as in the main paper Table. 3). We demonstrate the three components of PLUTO, namely, module selection, sharpness-aware pseudo-label entropy minimization (SA), and high-entropy sample filtering, through ablation experiments, highlighting their contributions to domain adaptation. It is evident that SA and Filter, in addition to module selection, contribute to the improved performance of PLUTO.

B. Parameter efficiency

Parameter-efficient tuning (PET) methods align naturally with model ensemble techniques (Lester et al., 2021), particularly in terms of parameter efficiency. In contrast to other models where an ensemble of N models results in N times more model parameters, an ensemble of N distinct PET modules merely entails N times more modules. This is because all models to be ensembled share the same pre-trained model that conditions the PET modules. Therefore,

although PLUTO is model ensemble test-time adaptation approach, the additional model parameters introduced by the ensemble are only the PET modules, i.e. $N \times |\theta|$. In our approach, we train an attention-based module selector \mathcal{G} which includes four projection layers and two layer norms. It required $d \times d'_x + d'_x \times d' + v \times d'_l + d'_l \times d' + 4d'$ parameters ($\approx 0.8M$ in our experiment). It only required about less than 1% of a pretrained ViT-base model ($\approx 86M$, Table. B).

C. Details on different PET methods

C.1. Visual-Prompt Tuning (VPT)

With a pre-trained Transformer (ViT) model as our starting point, we introduce a set of p continuous embeddings in the input space, each of dimension d , referred to as "prompts." During fine-tuning, only the prompts specific to the task are updated, while the Transformer backbone remains frozen. We applied VPT-Shallow(Jia et al., 2022) as following:

VPT-Shallow. Prompts are inserted into the first Transformer layer only. Each prompt token is a learnable d -dimensional vector. A module, which is a collection of p (which is the prompt length) prompts is denoted as $\mathbf{P} = \{\mathbf{v} \in \mathbb{R}^d | k \in \mathbf{N}, 1 \leq k \leq p\}$, the shallow-prompted ViT is:

$$[x_1, \mathbf{Z}_1, \mathbf{E}_1] = L_1([x_0, \mathbf{P}, \mathbf{E}_0]) \quad (\text{A})$$

$$[x_i, \mathbf{Z}_i, \mathbf{E}_i] = L_i([x_{i-1}, \mathbf{Z}_{i-1}, \mathbf{E}_{i-1}]), i = 2, \dots, l \quad (\text{B})$$

$$\mathbf{y} = \text{Head}(x_l), \quad (\text{C})$$

where $\mathbf{Z}_i \in \mathbb{R}^{p \times d}$ represents the features computed by the i -th Transformer layer, and $[x_i, \mathbf{Z}_i, \mathbf{E}_i] \in \mathbb{R}^{(1+p+P) \times d}$ (P is the number of patches that a 2D image input is divided into). The color above indicate **learnable** and **frozen** parameters, respectively. For ViTs, x_i is invariant to the location of prompts since they are inserted after positional encoding. The overall parameter count for Adapters in an l -layer Transformer can be calculated as $|\theta| = p \times d$.

C.2. Adapter

In the conventional configuration, a transformer model incorporates two Adapters per layer (Baevski & Auli, 2018). Each Adapter layer is composed of $2 \times k \times d$ parameters, accounting for both the down and up-projection matrices. Here, k represents the input dimension size, while d refers to the bottleneck dimension of the Adapter. The overall parameter count for Adapters in an l -layer Transformer can be calculated as $|\theta| = 2 \times l \times 2 \times k \times d$.

C.3. Results for different PET modules

Following the setup in main paper Sec. 4.3, we replace VPT with Adapters as the PET module, and demonstrate

Table C. **Results on Office-Home.** We train the source modules using 3 datasets to perform inference on the remaining dataset ($M = N = 3$). The difference here is that we applied Adapter instead of VPT in the main paper.

Source	Method	Ar	Cl	Pr	Re	Avg
Single	TENT-Best	65.6	52	77.9	72.1	66.9
	TENT-Worst	47.5	47.1	57.6	65.3	54.4
	CoTTA-Best	65.3	50.9	75.8	70.9	65.7
	CoTTA-Worst	46.6	46.2	56.1	63.8	53.2
	EaTA-Best	65.5	51.8	76.6	72.0	66.5
	EaTA-Worst	46.7	46.3	55.2	61.9	52.5
Multi	TENT-Ens	63.1	49.2	76.6	72.9	65.5
	CoTTA-Ens	65.4	49.9	77.2	71.8	66.1
	EaTA-Ens	65.2	50.7	76.3	71.6	66.0
	PLUTO (Ours)	65.7	55.4	79.1	77.1	69.3

Table D. **Results on Digits.** We train the source modules using 4 digits datasets to perform inference on the remaining dataset ($M = N = 4$). The difference here is that we applied Adapter instead of VPT in the main paper.

Source	Method	MM	MT	UP	SV	SY	Avg
Single	TENT-Best	54.5	97.6	83.7	86.6	94.5	83.4
	TENT-Worst	16.4	54.0	59.2	11.7	15.7	31.4
	CoTTA-Best	53.5	98.5	85.8	84.8	94.5	83.4
	CoTTA-Worst	16.2	53.9	58.6	10.3	16.3	31.1
	EaTA-Best	55.4	97.4	83.6	85.9	92.8	83.0
	EaTA-Worst	16.9	51.7	57.9	8.7	16.5	30.3
Multi	TENT-Ens	61.8	98.8	85.8	53.2	77.1	75.3
	CoTTA-Ens	56.2	98.6	85.5	87.0	95.3	84.5
	EaTA-Ens	56.3	96.7	83.8	86.4	94.5	83.5
	PLUTO (Ours)	64.0	99.1	89.9	87.3	95.5	87.2

the stationary distribution adaptation results in Table. C and Table. D. In can be concluded that our method, PLUTO, remains good performance across different PET modules.

D. Hyperparameters

The experimental setup of the attention-based module selector \mathcal{G} is listed as in Table. E. Table. F summarizes the optimization configurations we used. Implementation details for each tuning method on source/target tasks are also included.

E. Details of dataset corruptions

We summarize these corruptions types by example in Fig. A. The order of these corruptions is same as the order in Table. 6 and Table. 7

Table E. Hyperparameters of the module selector \mathcal{G} for different datasets.

Model	Hyper-param	CIFAR100-C	ImageNet-C	Office-Home	5-Digits
ViT-Base	d'_x	64	128	32	32
	d'_l	64	128	32	32
	d'	64	128	64	32
	Dropout %	0	0	0	50

Table F. Hyperparameters and implementation details for each tuning methods.

	Full, Adapter	VPT
Optimizer	AdamW	SGD
Optimizer momentum	N/A	0.9
$base_lr$ search range	{0.001, 0.0001, 0.0005, 0.005}	{50., 25., 10., 5., 2.5, 1., 0.5, 0.25, 0.1, 0.05}
Weight decay range	{0.01, 0.001, 0.0001, 0.0}	
LR schedule	cosine decay	
Warm up epochs	10	
Total epochs	100	

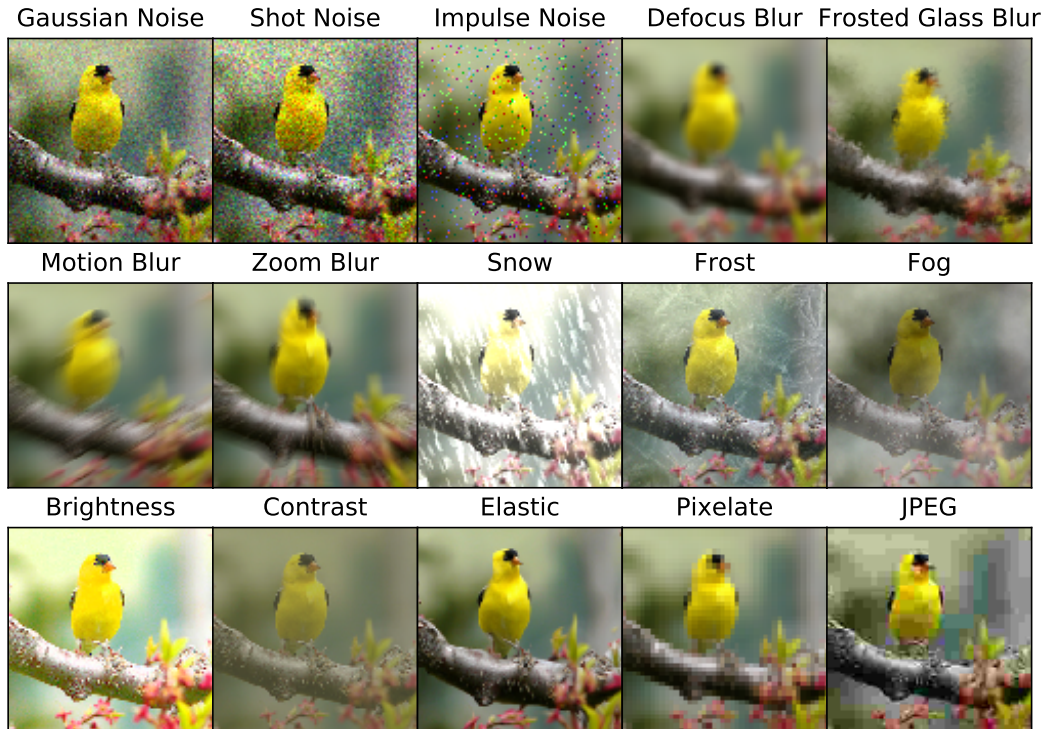


Figure A. Examples of each corruption type in the image corruptions benchmark. While synthetic, this set of corruptions aims to represent natural factors of variation like noise, blur, weather, and digital imaging effects.

F. Theoretical Insights

PLUTO’s goal is to determine the ideal weights $\{w(x)^j\}_{j=1}^N$ for every source, combining them to create the target predictor. We will demonstrate that, given logical assumptions about the source and target distributions, there is a straightforward selection of the target predictor. This selection can match or surpass the performance of the best source model when applied directly to the target data.

Formally, consider L as a convex loss function that maps a pair consisting of a model-predicted label and the actual ground-truth label to a scalar value. Let the expected loss over the k -th source distribution Q_S^k , utilizing the source predictor θ , be denoted as $\mathcal{L} = \mathbb{E}_x[L(\theta(x), y)]$, which can also be expressed as $\int_x L(\theta(x), y)Q_S^k(x)dx$. If the target distribution can be expressed by an linear combination of source distributions, i.e. $Q_T(x) = \sum_{k=1}^N \lambda_k Q_S^k(x)$, $\lambda_k \geq 0$, $\sum_{k=1}^N \lambda_k = 1$, and the source predictors are trained/finetuned to be optimal:

$$\theta_S^k = \operatorname{argmin}_{\theta} \mathcal{L}(Q_S^k, \theta), \forall 1 \leq k \leq N,$$

then the target predictor can be expressed as

$$\theta_T(x) = \sum_{k=1}^N \frac{\lambda_k Q_S^k(x)}{\sum_{j=1}^N \lambda_j Q_S^j(x)} \theta_S^k(x).$$

By applying Lemma 1,2 in (Ahmed et al., 2021), we can know that the pseudo-label loss (Eqn. 2) and the supervised loss are both less than or equal to the loss induced by the best source predictor, i.e.

$$\mathcal{L}(Q_T, \theta_T) \leq \min_{1 \leq j \leq N} \mathcal{L}(Q_T, \theta_S^j).$$

Which is consistent with the results shown in Table. 2, 3.